


## RESEARCH ARTICLE

# Effect of Fe<sub>2</sub>O<sub>3</sub> on steam gasification of subbituminous coal/woody biomass mixture

Lingbo Shen\* , Ayano Nakamura & Kenji Murakami

Department of Material Science, Faculty of Engineering and Resource Science, Akita University, 1-1 Tegata Gakuen-machi, Akita City 010-8502, Japan

**Keywords**

Co-gasification, iron catalyst, low-rank coal, woody biomass

**Correspondence**

Lingbo Shen, Department of Material Science, Faculty of Engineering and Resource Science, Akita University, 1-1 Tegata Gakuen-machi, Akita City 010-8502, Japan. E-mail: bobo198743@yahoo.co.jp

**Funding Information**

No funding information provided.

Received: 29 October 2017; Revised: 15 March 2018; Accepted: 17 April 2018

**Energy Science and Engineering** 2018; 6(4): 281–288

doi: 10.1002/ese3.193

**Abstract**

This study investigated the steam gasification of Indonesian Adaro coal and Japanese cedar mixed in a 1:1 ratio with the physical addition of 10 wt% Fe<sub>2</sub>O<sub>3</sub> in 50 vol% H<sub>2</sub>O at ambient atmospheric pressure and 800°C for 1 h. The primary objective of this work was to examine the effectiveness of an iron catalyst on the interaction between Indonesian Adaro coal and Japanese cedar. The study demonstrated that the H<sub>2</sub> evolution amount for co-gasification of Japanese cedar and Adaro coal (with 1:1 ratio in weight) without a Fe catalyst was 100 mmol/g-char. However, the H<sub>2</sub> evolution amount for co-gasification with the addition of Fe<sub>2</sub>O<sub>3</sub> was 152 mmol/g-char. The increase in the co-gasification for H<sub>2</sub> evolution was based on a change in the char structure during pyrolysis and gasification.

**Introduction**

As a renewable energy, biomass has gained importance with the development of a serious energy crisis and increased environmental challenges. Co-gasification of coal and biomass is one of the most practical means of converting these fuels into clean gas for use as a fuel or a chemical precursor. This is because co-gasification has several advantages [1–4]: for example, the addition of biomass to coal can reduce CO<sub>2</sub> emissions and the problems caused by the harmful ash contained in coal. However, high cost for biomass processing, transportation, and drying, and large amount of tar generation are big problems for biomass utilization. Coal mixing is regarded as a good solution to solve the problems. On the other hand, biomass has a different H/C and O/C molar ratio than coal leading to different reactivity and thermal characteristics

during co-gasification. For example, biomass with a high molar ratio of H/C may act as H<sub>2</sub> donors during copyrolysis of biomass and coal blends. Therefore, some synergistic effect producing more volatile products may occur [5–7].

Many researchers have also studied the effect of alkali metal and alkaline earth metal (AAEM) in biomass ash on co-gasification [8–10]. Wei et al. [8] concluded that AAEM in biomass ash, particularly K, can promote gasification and transform from biomass to another feedstock. Zhang et al. [9] performed experimentation on petroleum coke and corn cob co-gasification using thermogravimetric analysis (TGA). This study concluded that AAEM in biomass ash led to the promoted effect in co-gasification process. However, a high AAEM content in biomass feedstock resulted in serious challenges, such as ash slagging, fouling, agglomeration, deposition, and heated side corrosion

in a high-temperature environment [11–14]. Based on the work mentioned above, woody biomass with less ash was added to coal for co-gasification in recent years. For example, Adeyemi et al. [15] compared gasification behavior of coal and woody biomass and concluded that Kentucky coal produced higher gasification efficiency than wood. Zhang and Zheng [16] conducted co-gasification experimentation of two types of biomass (one was woody biomass) and coal determining that the ash in woody biomass could bring a promoted effect on promoting gasification reactivity of coal char. They also discussed the difference between fuel mixture (coal and woody biomass mixture) and fuel separation for gasification in another paper [16], which expressed that fuel mixture showed a much bigger synergy degree than that of fuel separation.

In previous study, iron-loaded biochar was used and shown to increase gasification of AD by 20% when compared to a coal sample with the same amount of iron catalyst. As such, iron-loaded biochar can be used as raw sample and as catalyst for gasification [17]. In this method, the iron-loaded biochar must be initially prepared with the iron catalyst loaded with impregnation. From a practical perspective, an easy and low-cost operation was selected. Thus, development of a co-gasification process for direct application in a coal/woody biomass is necessary.

This study investigates the co-gasification of biomass and AD coal without catalyst and with an iron catalyst. With a limited number of studies on catalytic co-gasification, the effect of an iron catalyst addition on the change in synergy (interaction between biomass and AD coal) was unknown. Hence, this study focused on the effect of iron catalyst on the interaction between biomass and AD coal.

## Experimental

### Samples

Indonesian Adaro subbituminous coal (AD) and Japanese cedar (SG) were used as coal and biomass samples, respectively. The particle size, the proximate, and the ultimate analyses were identical to our previous studies [17] as shown in Tables 1 and 2. The iron species was a commercial  $\text{Fe}_2\text{O}_3$  ( $\alpha\text{-Fe}_2\text{O}_3$ ).

### Preparation of mixed samples and iron catalyst loading

AD and SG were mixed in a mortar with a weight ratio of 1:1. After mixing the samples were stored in hermetic bags and labeled (SG+AD).

A physical mixing method was used for iron catalyst loading. To maintain a weight fraction of 10% loading,

**Table 1.** Proximate and ultimate analyses of AD.

Prox. analysis wt% (dry)			Ultimate analysis wt% (daf)				
Ash	VM	FC	C	H	N	S	O(diff.)
2.5	46.7	50.8	67.8	5.1	0.44	0.14	26.5

Particle size: 150–250  $\mu\text{m}$ .

**Table 2.** Proximate and ultimate analyses of SG.

Prox. analysis wt% (dry)			Ultimate analysis wt% (daf)			
Ash	VM	FC	C	H	N	O(diff)
0.9	78.4	20.7	46.9	5.8	0.1	46.2

Particle size: <250  $\mu\text{m}$ .

an applicable amount of iron species was added into AD, SG, and the mixed samples. The samples were mixed thoroughly, then labeled  $\text{Fe}_2\text{O}_3\text{-SG}$ ,  $\text{Fe}_2\text{O}_3\text{-AD}$ , and  $\text{Fe}_2\text{O}_3\text{-(SG+AD)}$ .

## Pyrolysis and steam gasification

The fixed-bed reactor used in this study, as shown in Figure 1, is identical to the reactor in previous work published by Shen and Murakami [17]. Initially, approximately 0.5 g of one sample was placed on quartz wool in the center of the vertical fixed-bed-type reactor. The sample was heated from room temperature to 800°C at a heating rate of 300°C/min under a flowing He gas rate of 140 mL/min, at which it was then maintained for 10 min. The char was weighed and its yield was calculated using the following equation:

$$Y_{\text{char}} = \frac{M_{\text{char}}}{M_{\text{sample}}} \quad (1)$$

where  $Y_{\text{char}}$  is the weight ratio of char yield and  $M_{\text{char}}$  is the weight of char [g(dried, ash and catalyst free)].  $M_{\text{sample}}$  is the weight of the sample [g(dried, ash and catalyst free)].

After a 10 min pyrolysis, the char was maintained in a volume ratio of 50%  $\text{H}_2\text{O}/\text{He}$  for 60 min. With a MicroGC and flowmeter the gas evolution rate was calculated using the following equation:

$$R = \frac{V_{\text{vol}}\% \times L}{22.4 \times M_{\text{char}}} \quad (2)$$

where  $R$  is the gas evolution rate [mmol/g-char-min],  $V_{\text{vol}}\%$  is the volume fraction of each produced gas measured by the MicroGC, and  $L$  is the total gas flow rate [mL/min].  $M_{\text{char}}$  is the weight of char [g].

Carbon conversion could be explained as the ratio of the amount of carbon evolved as gases to the amount

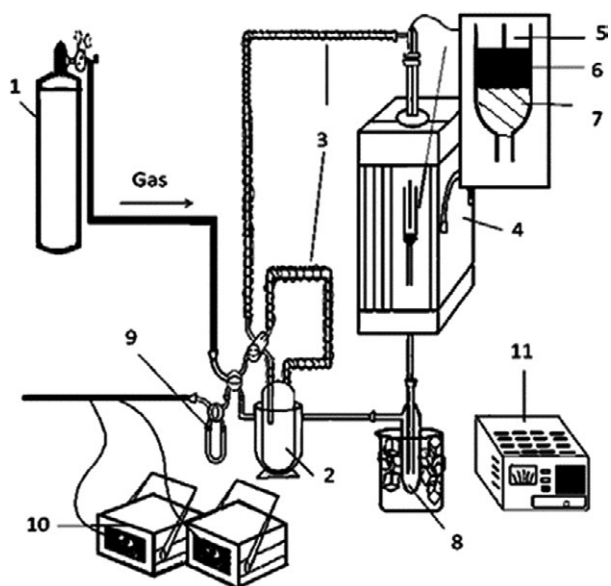


**Figure 1.** Fixed bed reactor for pyrolysis and steam gasification. 1. Carrier gas, 2. Steam generator, 3. Ribbon heater, 4. Electric furnace, 5. Thermocouple, 6. Sample, 7. Quartz wool, 8. Tar trap, 9. Dehydrating agent, 10. MicroGC, and 11. Temperature controller.

of carbon present in the char before gasification. It could be calculated using the following equation:

$$X_{\text{Carbon}} = \frac{C_{\text{gas}}}{C_{\text{Char}}} \quad (3)$$

where  $X_{\text{Carbon}}$  is the carbon conversion,  $C_{\text{gas}}$  is the total mol content of carbon-containing gases (the sum of  $\text{CO}$ ,  $\text{CO}_2$ ,  $\text{CH}_4$ ,  $\text{C}_2\text{H}_4$ , and  $\text{C}_2\text{H}_6$  mol content), and  $C_{\text{char}}$  is the mol content of carbon in the char, in which the char was assumed to be 100% carbon.

## Characterization of the pyrolyzed char and gasified residue

The form of iron catalyst after pyrolysis and steam gasification was measured by XRD under conditions that were identical to what was previously reported [17].

## Result and Discussion

### The hydrogen evolution profiles for co-gasification of AD and SG

Figure 2 shows the hydrogen evolution profiles for Adaro coal and cedar mixture (SG+AD) with and without  $\text{Fe}_2\text{O}_3$ . As noted in this figure, the addition of  $\text{Fe}_2\text{O}_3$  had a higher hydrogen rate than (SG+AD). ( $\text{Fe}_2\text{O}_3$ -SG+ $\text{Fe}_2\text{O}_3$ -AD) showed the sum of the hydrogen rate for independent gasification of  $\text{Fe}_2\text{O}_3$ -SG and  $\text{Fe}_2\text{O}_3$ -AD, which

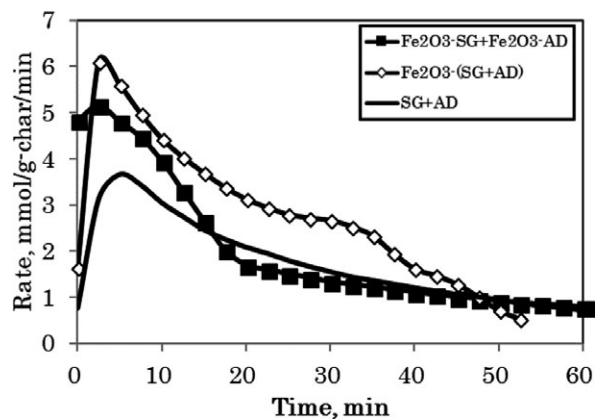


**Figure 2.** The hydrogen evolution rates for co-gasification of SG and AD mixture with and without  $\text{Fe}_2\text{O}_3$ .

did not contain the interaction of  $\text{Fe}_2\text{O}_3$ -SG and  $\text{Fe}_2\text{O}_3$ -AD. Comparing  $\text{Fe}_2\text{O}_3$ -(SG+AD) with ( $\text{Fe}_2\text{O}_3$ -SG+ $\text{Fe}_2\text{O}_3$ -AD) in Figure 2, allowed observing a significant increase in the center of the time range.

As reported in the previous study [17], the main reactions under the conditions should be as follows:

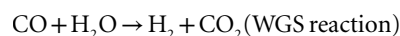
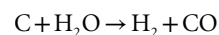


Table 3 shows the amount of  $\text{H}_2$ ,  $\text{CO}_2$ ,  $\text{CO}$ , and ratio of  $\text{H}_2/\text{CO}$  for (SG+AD) and  $\text{Fe}_2\text{O}_3$ -(SG+AD). From Table 3, amount of  $\text{H}_2$  and  $\text{CO}_2$  largely increased after  $\text{Fe}_2\text{O}_3$  added, moreover, ratio of  $\text{H}_2/\text{CO}$  also increased from 7.1 to 13.8. Thus,  $\text{Fe}_2\text{O}_3$  addition promoted WGS reaction in the steam gasification.

### Synergy in noncatalyst co-gasification and catalytic co-gasification

Synergy is the interaction between biomass and coal. Moreover, the synergy may be facilitation, but also may be an inhibition for gasification reaction. Therefore, for co-gasification it is important to know if a promoted synergistic effect existed.

In this study, the experimental amount of hydrogen evolution was compared with a calculated value to determine synergy. Equation 4 was used to calculate the value for co-gasification without a catalyst.

$$\text{Amount(cal)} = \frac{\text{Amount(AD)} \times M(\text{ADchar}) + \text{Amount(SG)} \times M(\text{SGchar})}{M(\text{ADchar}) + M(\text{SGchar})} \quad (4)$$

where Amount(AD) is the amount of hydrogen evolution for 1 g of ADchar; Amount(SG) is the amount of

**Table 3.** Amount of H<sub>2</sub>, CO<sub>2</sub>, CO, and ratio of H<sub>2</sub>/CO for (SG+AD) and Fe<sub>2</sub>O<sub>3</sub>-(SG+AD) during 60 min gasification.

	H <sub>2</sub> (mmol/g-char)	CO <sub>2</sub> (mmol/g-char)	CO (mmol/g-char)	H <sub>2</sub> /CO
SG+AD	100	44	14	7.1
Fe <sub>2</sub> O <sub>3</sub> -(SG+AD)	152	71	11	13.8

hydrogen evolution for 1 g of SGchar; and M(ADchar) and M(SGchar) are weights of ADchar and SGchar, respectively.

For co-gasification with Fe<sub>2</sub>O<sub>3</sub> Equation (5) was used.

$$\text{Amonut (cal)} = \frac{\text{Amount (FeAD)} \times \text{M(FeADchar)} + \text{Amount (FeSG)} \times \text{M(FeSGchar)}}{\text{M(FeADchar)} + \text{M(FeSGchar)}} \quad (5)$$

where Amount(FeAD) is the amount of hydrogen evolution for 1 g of Fe<sub>2</sub>O<sub>3</sub>-AD char; Amount(FeSG) is the amount of hydrogen evolution for 1 g of Fe<sub>2</sub>O<sub>3</sub>-SG char; and M(FeADchar) and M(FeSGchar) are weights of Fe<sub>2</sub>O<sub>3</sub>-ADchar and Fe<sub>2</sub>O<sub>3</sub>-SGchar, respectively.

Figure 3 shows the comparison of the experimental and calculated amount of hydrogen evolution for co-gasification. For co-gasification without catalyst, the experimental amount of (SG+AD) is 100 mmol/g-char while the calculated amount is 85 mmol/g-char. Therefore, the synergy for (SG+AD) results in a 15 mmol/g-char increase in H<sub>2</sub>.

For co-gasification after added Fe<sub>2</sub>O<sub>3</sub>, the experimental H<sub>2</sub> amount of Fe<sub>2</sub>O<sub>3</sub>-(SG+AD) is 152 mmol/g-char and the calculated H<sub>2</sub> amount is 121 mmol/g-char. Therefore, the synergy for Fe<sub>2</sub>O<sub>3</sub>-(SG+AD) results in a 31 mmol/g-char increase in H<sub>2</sub>, which is significantly higher than the synergy of (SG+AD) without catalyst.

### Effect of Iron on reactivity of char for co-gasification

Specific rate, as calculated by equation (6), is used to compare the change in reaction activity as well as degree of reactivity.

$$R_s = \frac{R_c}{W_{sc}} \quad (6)$$

where  $R_s$  is the specific rate [1/h],  $R_c$  is the rate of carbon conversion [mol%/h], and  $W_{sc}$  is the amount of residual carbon in the char [mol%].

As illustrated in Figure 4, the specific rate of (SG+AD) without iron catalyst is nearly constant during the complete gasification process. With the addition of Fe<sub>2</sub>O<sub>3</sub>, the specific rate of Fe<sub>2</sub>O<sub>3</sub>-(SG+AD) increased with increased carbon conversion. A continuing promoting effect was noted after the addition of Fe<sub>2</sub>O<sub>3</sub>. However, the specific rate of (Fe<sub>2</sub>O<sub>3</sub>-SG+Fe<sub>2</sub>O<sub>3</sub>-AD) increased initially then

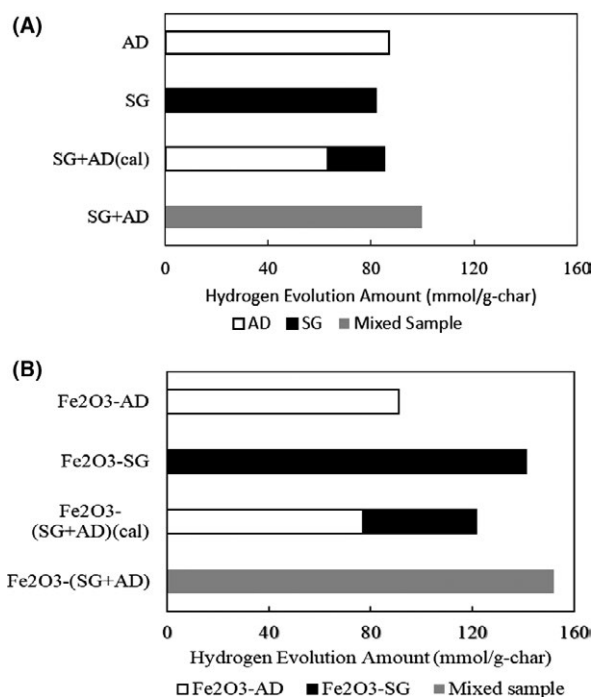


**Figure 3.** Comparison of the experimental amount and calculated amount of hydrogen evolution for co-gasification of SG and AD mixture (A) Without Fe<sub>2</sub>O<sub>3</sub>, (B) With Fe<sub>2</sub>O<sub>3</sub>.

decreased similar to the change in Fe<sub>2</sub>O<sub>3</sub>-AD. This indicated that SG addition increased the Fe catalyst effect on char reactivity, which resulted in the difference of specific rate.

### Change with Fe<sub>2</sub>O<sub>3</sub> addition during pyrolysis

Figure 5 shows the difference between samples with and without Fe<sub>2</sub>O<sub>3</sub> during pyrolysis. In all samples, the weight of char for the samples with the catalyst at 800°C was higher than for the samples without Fe<sub>2</sub>O<sub>3</sub>. However, a difference in reaction temperature was noted between the samples such that for Fe<sub>2</sub>O<sub>3</sub>-AD and AD, the change began at 480°C. The change began at approximately 250°C for Fe<sub>2</sub>O<sub>3</sub>-(SG+AD) and (SG+AD). Therefore, in Fe<sub>2</sub>O<sub>3</sub>-(SG+AD), the Fe catalyst reacted at a relatively low temperature. A similar result was reported in Zhang et al.'s study [18], in this case, iron catalyst was considered to be coordinated to a range of oxygen-containing ligands in coal or biomass, including O<sub>2</sub><sup>-</sup>, OH<sup>-</sup>, and COO<sup>-</sup>, which

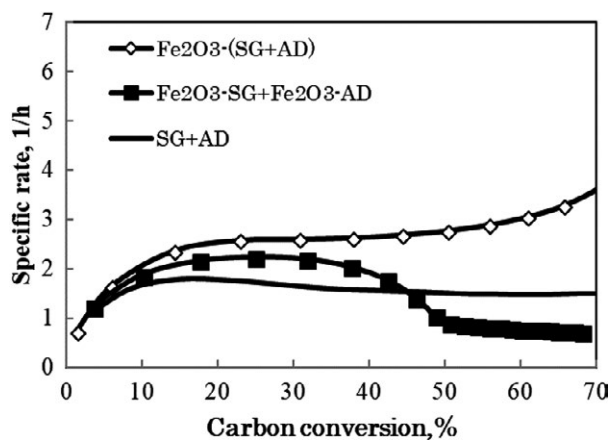


Figure 4. Influence on specific rate for (SG+AD) after mixed  $\text{Fe}_2\text{O}_3$ .

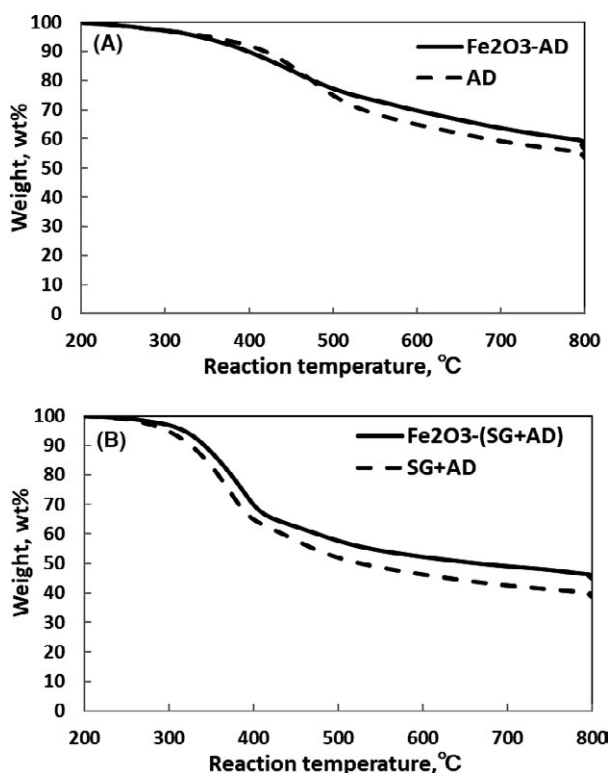


Figure 5. The difference between samples with and without  $\text{Fe}_2\text{O}_3$  during pyrolysis (A) AD with and without 10 wt%  $\text{Fe}_2\text{O}_3$  loading, (B) (SG+AD) with and without 10 wt%  $\text{Fe}_2\text{O}_3$  loading.

were generally associated with tar precursors. In our study, SG produced a large amount of tar during pyrolysis, this may be an important reason why the difference appeared after SG added.

Figure 6 shows TG and DTG as a comparison of experimental and calculated values for iron-loaded samples.  $\text{Fe}_2\text{O}_3$ -(SG+AD)cal, which is the calculated value, was utilized for comparison to  $\text{Fe}_2\text{O}_3$ -(SG+AD). The weight

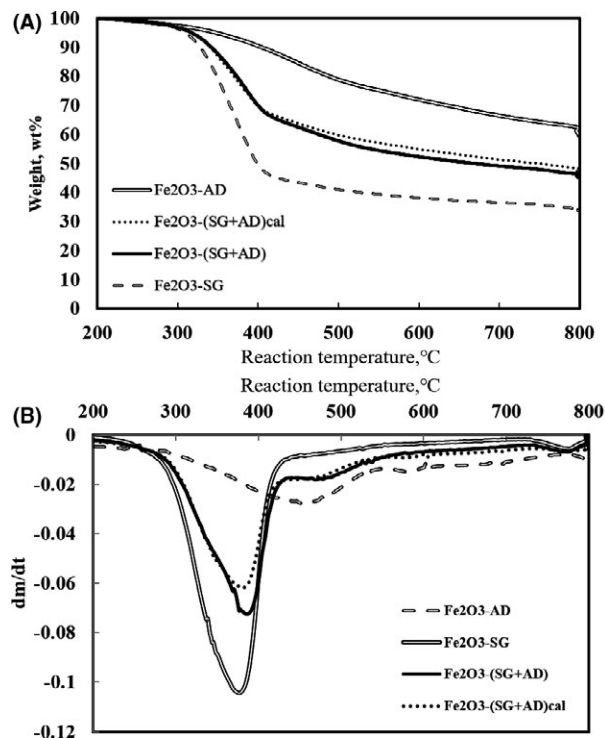


Figure 6. Comparison of experimental and calculated values for iron-loaded samples with TG and DTG.

of  $\text{Fe}_2\text{O}_3$ -(SG+AD)cal and  $(dm/dt)$  of  $\text{Fe}_2\text{O}_3$ -(SG+AD)cal was calculated as from Equations (7) and (8).

$$W_{\text{Fe}_2\text{O}_3\text{-(SG+AD)cal}} = 1/2W_{\text{Fe}_2\text{O}_3\text{-SG}} + 1/2W_{\text{Fe}_2\text{O}_3\text{-AD}} \quad (7)$$

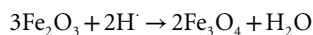
$$\begin{aligned} (dm/dt)_{\text{Fe}_2\text{O}_3\text{-(SG+AD)cal}} = \\ 1/2(dm/dt)_{\text{Fe}_2\text{O}_3\text{-SG}} + 1/2(dm/dt)_{\text{Fe}_2\text{O}_3\text{-AD}} \end{aligned} \quad (8)$$

The significant mass loss for  $\text{Fe}_2\text{O}_3$ -(SG+AD) and  $\text{Fe}_2\text{O}_3$ -(SG+AD)cal occurred between 300°C and 430°C. At this temperature range, the coal and biomass cracked into small fragments. Comparing  $\text{Fe}_2\text{O}_3$ -(SG+AD) with  $\text{Fe}_2\text{O}_3$ -(SG+AD)cal, the primary mass loss for  $\text{Fe}_2\text{O}_3$ -(SG+AD) was larger than for  $\text{Fe}_2\text{O}_3$ -(SG+AD)cal during the pyrolysis shown in Figure 6(B) indicating that cracking of  $\text{Fe}_2\text{O}_3$ -AD was promoted. Above 430°C, a condensation reaction was the primary reaction.  $W_{\text{Fe}_2\text{O}_3\text{-(SG+AD)}}$  was gradually lower than  $W_{\text{Fe}_2\text{O}_3\text{-(SG+AD)cal}}$  as shown in Figure 6(A), indicating that the condensation reaction for  $\text{Fe}_2\text{O}_3$ -AD was suppressed.

Figure 7 shows the XRD patterns of a  $\text{Fe}_2\text{O}_3$ -loaded sample during pyrolysis. From the TG in Figure 6(B) it can be concluded that the cracking reaction was essentially complete at approximately 500°C. Fe catalyst remained as  $\text{Fe}_3\text{O}_4$  and  $\text{Fe}_2\text{O}_3$  in  $\text{Fe}_2\text{O}_3$ -(SG+AD); and

$\text{Fe}_2\text{O}_3$  in  $\text{Fe}_2\text{O}_3$ -AD. Above  $800^\circ\text{C}$  the Fe catalyst was reduced to FeO and  $\alpha$ -Fe in  $\text{Fe}_2\text{O}_3$ -(SG+AD); and FeO in  $\text{Fe}_2\text{O}_3$ -AD. At  $800^\circ\text{C}$  for 10 min, the Fe catalyst remained as  $\alpha$ -Fe and Fe-C (Austenite) in  $\text{Fe}_2\text{O}_3$ -AD and  $\text{Fe}_2\text{O}_3$ -(SG+AD).

In the cracking stage ( $<500^\circ\text{C}$ ), the release of tar significantly contributed to the sample weight loss. Tar may have been produced by the release of the small fragments in the coal or biomass with hydrogen radicals.  $\text{Fe}_2\text{O}_3$  could react with hydrogen radicals as below.



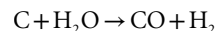
This is probably the reason why  $\text{Fe}_2\text{O}_3$  in  $\text{Fe}_2\text{O}_3$ -(SG+AD) could be reduced at this temperature range. SG released active H not only reducing  $\text{Fe}_2\text{O}_3$  to  $\text{Fe}_3\text{O}_4$  but also reacting with AD coal and promoting AD coal cracking (Fig. 6A). For the  $\text{Fe}_2\text{O}_3$ -AD sample, the weight of char only changed slightly as shown in Figure 6(A) and  $\text{Fe}_2\text{O}_3$  was not reduced (Fig. 7A) indicating that the effect of Fe catalyst was minor at this stage. This may be because AD coal lacks volatile matters (most of H, O, and volatile carbon) while SG maintains a large amount of volatile matters. As the temperature increased above  $500^\circ\text{C}$ , the intermediate products ( $-\text{COOFe}$  and  $-\text{COFe}$ ) continued to participate in the condensation and deoxidize reactions, forming new fixed carbon and increasing char weight. Then, Fe-O bonds disintegrated and resulted in the reduction of Fe catalyst. Thus, the iron catalyst remained as a reduced state of iron at last.

### Change during gasification

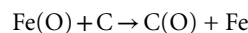
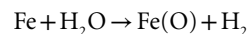
Figure 8 shows that the Fe catalyst changed from a reduced state ( $\alpha$ -Fe) to  $\text{Fe}_3\text{O}_4$  (oxidation state) for Fe-loaded

samples. This directly corresponded to the change Yu et al. [19] reported.

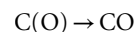
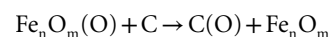
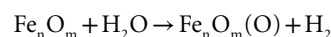
In the case of gasification without catalyst,



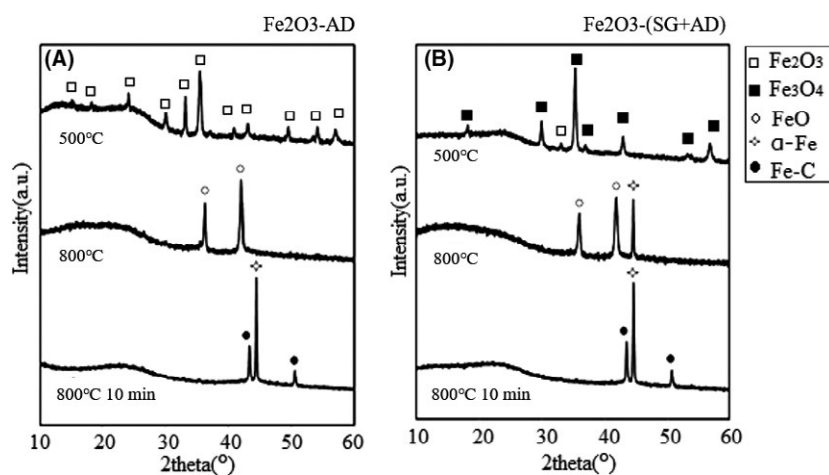
In the case of steam gasification by steam with Fe catalyst,



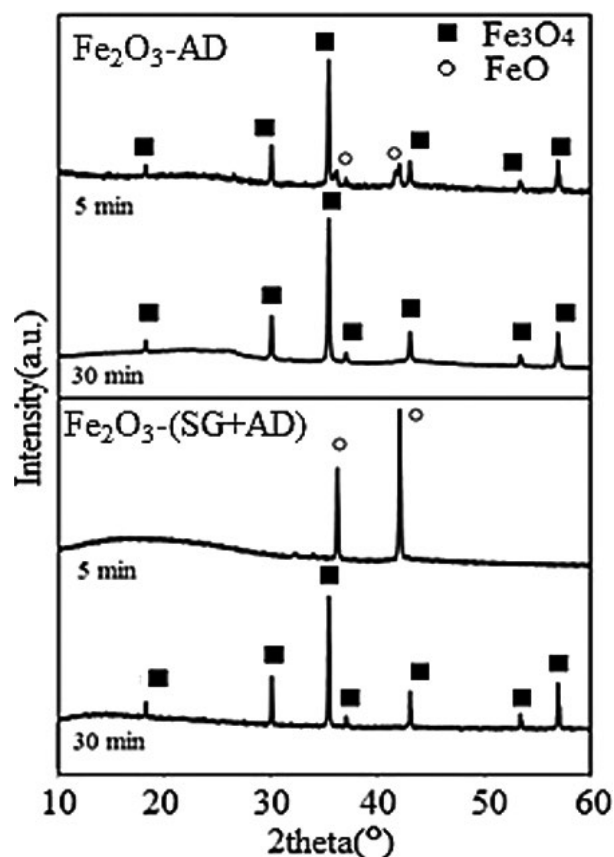
In the case of steam gasification with  $\text{Fe}_n\text{O}_m$ ,



Therefore, the Fe catalyst may have acted as an oxygen transfer agent in steam gasification as described by Yu et al. [19]. However, there was a difference between iron formed during gasification for different iron-loaded samples with a significant difference for the iron catalyst effect (Carbon conversion for  $\text{Fe}_2\text{O}_3$ -AD was 5% at 5 min and 38% at 30 min; Carbon conversion for  $\text{Fe}_2\text{O}_3$ -(SG+AD) was 6% at 5 min and 70% at 30 min). SG addition changed the effect of Fe catalyst. This indicated that when the Fe catalyst reacted with  $\text{H}_2\text{O}$  into Fe(O), the Fe(O) successfully transferred oxygen to carbon. This may have resulted from the change between the Fe catalyst and char during pyrolysis.



**Figure 7.** XRD patterns of  $\text{Fe}_2\text{O}_3$ -loaded sample during pyrolysis. (A)  $\text{Fe}_2\text{O}_3$ -AD, (B)  $\text{Fe}_2\text{O}_3$ -(SG+AD).



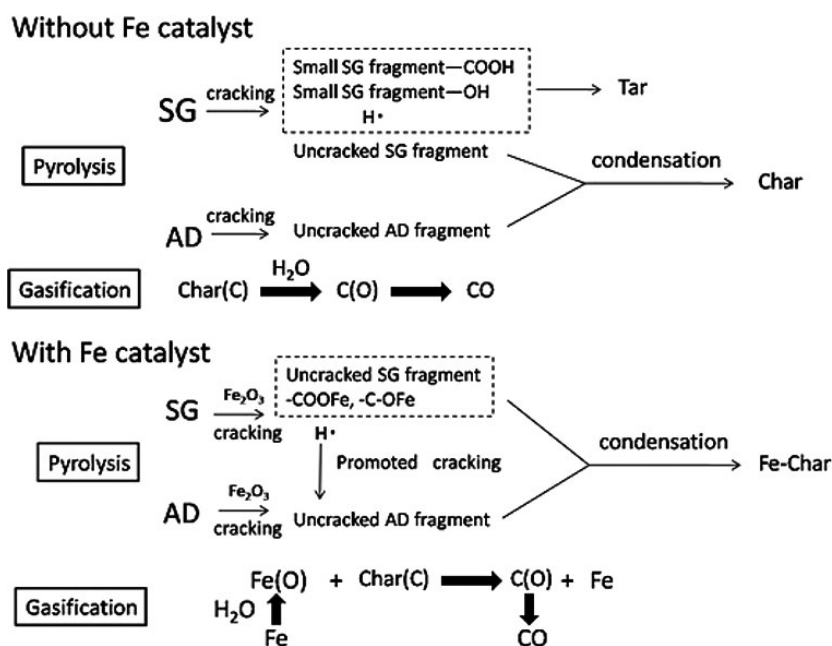
**Figure 8.** XRD patterns of  $\text{Fe}_2\text{O}_3\text{-AD}$  and  $\text{Fe}_2\text{O}_3\text{-(SG+AD)}$  after 5 and 30 min gasification at  $800^\circ\text{C}$ .

Figure 9 displays reactions in pyrolysis and gasification. As described above, in the noncatalyst case, SG initially cracked into small fragments and  $\text{H}^\cdot$  and then formed tar and uncracked SG fragments. AD cracked into uncracked AD fragments; then the uncracked SG fragments and uncracked AD fragments formed a condensate of char. For gasification, char reacted with  $\text{H}_2\text{O}$  producing  $\text{CO}$  and  $\text{H}_2$ . With the addition of  $\text{Fe}_2\text{O}_3$ , the Fe catalyst attached to a range of oxygen-containing ligands, including  $\text{O}^{2-}$ ,  $\text{OH}^-$ ,  $\text{COO}^-$ , and formed new fixed carbon at a low temperature. Additionally,  $\text{H}^\cdot$  from SG cracking reacted with uncracked AD fragments, promoting AD cracking. Subsequently, uncracked AD fragments, uncracked SG fragments, and newly formed fixed carbon formed a condensate of Fe-char, which supported contacting the Fe catalyst with carbon. For gasification, the Fe catalyst reacted with  $\text{H}_2\text{O}$  initially, keeping the oxygen from the  $\text{H}_2\text{O}$  and forming  $\text{Fe}(\text{O})$ . The  $\text{Fe}(\text{O})$  transferred the oxygen into carbon in the char, making gasification process easier for the catalyst samples.

With the SG and Fe catalyst, AD pyrolysis was changed, formed active carbon, and increased the reactivity of char. This is considered as an important reason for the increased synergy.

## Conclusion

This study conducted steam gasification of Indonesian Adaro coal (AD) and Japanese cedar (SG) at a ratio of 1:1 with the physical addition of a weight ratio of 10%



**Figure 9.** Reactions in pyrolysis and gasification with and without Fe catalyst.

Fe<sub>2</sub>O<sub>3</sub> in a volume ratio of 50% H<sub>2</sub>O at 800°C for 1 h. The conclusions are as follows:

1. The H<sub>2</sub> evolution for co-gasification without a Fe catalyst was 100 mmol/g-char, whereas H<sub>2</sub> evolution for co-gasification increased to 152 mmol/g-char with a catalyst.
2. Without an iron catalyst the specific rate of (SG+AD) remained nearly constant during the gasification process. Subsequent to the addition of Fe<sub>2</sub>O<sub>3</sub> the specific rate of Fe<sub>2</sub>O<sub>3</sub>-(SG+AD) increased with increased carbon conversion.
3. With a SG and Fe catalyst, the promotion of AD cracking and the formation of active carbon increased the reactivity of char.

## Conflict of Interest

None declared.

## References

1. Kazuhiro, K., H. Toshiaki, F. Shinji, M. Tomoaki, and S. Kinya. 2007. Co-gasification of woody biomass and coal with air and steam. *Fuel* 86:684–689.
2. Brown, C. R., Q. Liu, and G. Norton. 2000. Catalytic effects observed during the co-gasification of coal and switchgrass. *Biomass Bioenerg.* 18:499–506.
3. Chmielniak, T., and M. Sciazko. 2003. Co-gasification of biomass and coal for methanol synthesis. *Appl. Energy* 74:393–403.
4. Mclendon, T. R., A. P. Lui, R. L. Pineault, S. K. Beer, and S. W. Richardson. 2004. High-pressure co-gasification of coal and biomass in a fluidized bed. *Biomass Bioenerg.* 26:377–388.
5. Dong, K. P., D. K. Sang, H. K. See, and G. L. Jae. 2010. Co-pyrolysis characteristics of sawdust and coal blend in TGA and a fixed bed reactor. *Biores. Technol.* 101:6151–6156.
6. Zhang, L., S. P. Xu, W. Zhao, and S. Liu. 2007. Co-pyrolysis of biomass and coal in a free fall reactor. *Fuel* 86:353–359.
7. Haykiri-Acma, H., and S. Yaman. 2010. Interaction between biomass and different rank coals during co-pyrolysis. *Renew. Energy* 35:288–292.
8. Wei, J., Q. Guo, Y. Gong, L. Ding, and G. Yu. 2017. Synergistic effect on co-gasification reactivity of biomass-petroleum coke blended char. *Biores. Technol.* 234:33–39.
9. Zhang, Y., Y. Zheng, M. Yang, and Y. Song. 2016. Effect of fuel origin on synergy during co-gasification of biomass and coal in CO<sub>2</sub>. *Biores. Technol.* 200:789–794.
10. Zhang, Z., S. Pang, and T. Levi. 2017. Influence of AAEM species in coal and biomass on steam co-gasification of chars of blended coal and biomass. *Renew. Energy* 101:356–363.
11. Nutalapati, D., R. Gupta, B. Moghtaderi, and T. F. Wall. 2007. Assessing slagging and fouling during biomass combustion: a thermodynamic approach allowing for alkali/ash reactions. *Fuel Process. Technol.* 88:1044–1052.
12. Li, Q. H., Y. G. Zhang, A. H. Meng, and G. X. Li. 2013. Study on ash fusion temperature using original and simulated biomass ashes. *Fuel Process. Technol.* 88:107–112.
13. Pintana, P., and N. Tippayawong. 2016. Predicting Ash Deposit Tendency in Thermal Utilization of Biomass. *Eng. J.* 20:15–24.
14. Vélez, J. F., F. Chejne, C. F. Valdés, E. J. Emery, and C. A. Londoño. 2009. Co-gasification of Colombian coal and biomass in fluidized bed: an experimental study. *Fuel* 88:424–430.
15. Adeyemi, I., I. Janajreh, T. Arink, and C. Ghenai. 2017. Gasification behavior of coal and woody biomass: validation and parametrical study. *Appl. Energy* 185:1007–1018.
16. Zhang, Y., and Y. Zheng. 2016. Co-gasification of coal and biomass in a fixed bed reactor with separate and mixed bed configurations. *Fuel* 183:132–138.
17. Shen, L., and K. Murakami. 2016. Steam co-gasification of iron-loaded biochar and low-rank coal. *Int. J. Energy Res.* 40:1846–1854.
18. Zhang, F., D. Xu, Y. Wang, M. Argyle, and M. Fan. 2015. CO<sub>2</sub> gasification of Powder River Basin coal catalyzed by a cost-effective and environmentally friendly iron catalyst. *Appl. Energy* 145:295–305.
19. Yu, J. L., F. J. Tian, M. C. Chow, L. J. Mckenzie, and C. Z. Li. 2006. Effect of iron on the gasification of Victorian brown coal with steam: enhancement of hydrogen production. *Fuel* 85:127–133.